

Seismic fragility of typical bridges in moderate seismic zones

Eunsoo Choi, Reginald DesRoches*, Bryant Nielson

School of Civil and Environmental Engineering, Georgia Institute of Technology, Atlanta, GA 30332-0355, USA

Received 18 June 2003; accepted 15 September 2003

Abstract

A set of fragility curves for the bridges commonly found in the Central and Southeastern United States (CSUS) is presented. Using the results of an inventory analysis of the typical bridges in the CSUS, four typical bridge types are identified. Using non-linear analytical models, and a suite of synthetic ground motions, analytical fragility curves are developed for the four bridge types. The fragility curves were first generated for the individual components of each of the bridge types and then, they were combined into fragility curves that represent the entire bridge system using first-order reliability principles. The fragility curves show that the peak ground acceleration for a 50% probability of exceeding slight damage ranges from approximately 0.19 to 0.24 g for the four bridge types. Comparison of the fragility curves shows that the most vulnerable bridge types are the multi-span simply supported and multi-span continuous steel-girder bridges. The least vulnerable bridge is the multi-span continuous pre-stressed concrete-girder bridge. The developed fragility curves can be used for economic loss estimation as well as a basis for assigning retrofit prioritization for bridges. This is particularly useful in the Central and Southeastern United States where seismic retrofit of bridges is becoming more prevalent.

© 2003 Elsevier Ltd. All rights reserved.

Keywords: Fragility; Seismic; Bridges; Vulnerability; Retrofit; Moderate seismic zones

1. Introduction

An emerging tool in assessing the seismic vulnerability of highway bridges is the use of fragility curves. Fragility curves describe the probability of a structure being damaged beyond a specific damage state for various levels of ground shaking. This, in turn, can be used for prioritizing retrofit, pre-earthquake planning, and loss estimation tools. This is particularly useful in regions of moderate seismicity, such as the Central and Southeastern United States, where bridge officials are beginning to develop retrofit programs, in addition to conducting pre-earthquake planning. In light of the damage to bridges observed in recent earthquakes [1–6], there is a significant need to perform adequate assessment of the vulnerability of bridges and bridge networks prior to future seismic events.

Fragility curves can be either empirical or analytical. Empirical fragility curves are usually based on the reported bridge damage from past earthquakes. Basoz et al. [7] developed empirical fragility curves for the bridge damage resulting from the 1994 Northridge, CA earthquake using logistical regression analysis to account for uncertainties in the damage data. Shinozuka et al. [8] used the maximum likelihood method to generate the empirical fragility curves from the observations of bridge damage in the 1995 Kobe earthquake.

Analytical fragility curves are developed through seismic response data from the analysis of bridges. The fragility analysis generally includes three major parts: (a) the simulation of ground motions, (b) the simulation of bridges to account for uncertainty in bridge properties, and (c) the generation of fragility curves from the seismic response data of the bridges. The seismic response data can be obtained from nonlinear time history analysis [8–10], elastic spectral analysis [11], or nonlinear static analysis [12,13].

Comparisons of empirical and analytical fragility curves have shown good agreement between theory and

* Corresponding author. Tel.: +1-404-385-0826; fax: +1-404-894-0221.

E-mail address: reginald.desroches@ce.gatech.edu (R. DesRoches).

field observation for the 1994 Northridge, and 1989 Loma Prieta earthquakes [7,12]. However, empirical fragility curves which have been developed for bridges in California following the 1989 Loma Prieta earthquake and the 1994 Northridge earthquake are generally not applicable to bridges in the Central and Southeastern United States due to differences in ground motion and bridge characteristics. Therefore, to develop fragility curves for bridges in the CSUS, analytical methods must be used. In this study, fragility curves are developed for a class of bridges commonly found in the CSUS to assess the vulnerability of the bridges and assist in the prioritization of retrofit for these bridges. The fragility curves are developed by performing nonlinear time history analyses for four different classes of bridges. For each bridge type, 10 sample bridges, representing the variability in material properties, are developed. A set of 100 ground motion records, with varying magnitudes, distances, and peak ground accelerations, is used in the response history analysis. The fragility curves are developed for various damage states for the bearings and columns. These individual component fragilities are combined to provide an approximation to the overall system fragility curves.

2. Bridge characteristics

A detailed analysis of the bridge inventory in the Central and Southeastern United States, performed in a previous study, shows that approximately 95% of the bridges in the CSUS are multi-span simply supported girder bridges, multi-span continuous girder bridges, or single span bridges as seen in Table 1 [14]. The majority of these bridges have either reinforced concrete, pre-stressed concrete or steel girders with reinforced concrete decks as seen in Table 1 [14].

When attempting to generate fragility curves that are representative of a class of bridges, there are some generalizations that must be made. As-built bridge plans were collected from the various departments of transportation and examined to determine pier details, superstructure types and bearing types [14]. Although all details were not identical, the details used in this study were deemed representative of their respective bridge classes. The substructure of these bridges typi-

cally consists of concrete bent caps supported on multiple columns. Previous studies have shown that the single span bridges are highly resistant to seismic loading and therefore are not considered in this study [14]. Brief descriptions of the four bridge types that are used in this study are provided below.

2.1. Multi-span simply supported steel girder bridge

The typical multi-span simply supported bridge with steel girders (MSSS-SG) considered in this study is shown in Fig. 1. The bridge has three spans and two multi-column bents. Each bent has four columns and each span has 11 girders. The span lengths used in this analysis are 12.2, 24.4, and 12.2 m (40, 80, and 40 ft), respectively, and the width is 20.5 m (67.0 ft). The column height of the piers is 4.6 m (15 ft). A 20.5 m × 2.4 m (67 ft × 8 ft, W × H) pile bent abutment with 13 piles is used. The nominal gap between deck and abutment is 38.1 mm (1.5 in.) and the nominal gap between decks is 25.4 mm (1.0 in.). The concrete slabs of the MSSS bridges are supported by steel girders resting on steel bearings. The steel bearings are mounted on abutments and cap beams. Two adjacent decks are separated by expansion joints above the bents.

2.2. Multi-span continuous steel girder bridge

The multi-span continuous steel girder bridge (MSC-SG) is similar to the MSSS-SG bridge, except that the girders are continuous across the bent. The span lengths used in this analysis are 30.3 m (99.5 ft), 37.9 m (124.5 ft), and 32.8 m (107.5 ft), respectively. A 17.7 m (58 ft) wide bent cap is supported on four columns of approximate height, 4.9 m (16 ft). The decks are composite steel girders with a concrete slab. Fixed bearings are located on cap beams, and rocker bearings are located at the abutments providing expansion joints at these locations.

2.3. Multi-span simply supported pre-stressed concrete girder bridge

The multi-span simply supported pre-stressed concrete girder bridge (MSSS-PSC) consists of three sim-

Table 1
Inventory of bridges in mid-America [14]

Superstructure span type					Superstructure material					
Total	MSSS (%)	Single span (%)	MSC (%)	Other (%)	Total	Steel (%)	PSC (%)	RC (%)	Wood (%)	Other (%)
109 162 (100.0)	45 639 (41.8)	27 384 (25.1)	30 798 (28.2)	5341 (4.9)	109 162 (100.0)	30 221 (32.1)	19 155 (20.3)	41 080 (43.6)	3043 (4.0)	228 (0.0)

MSSS, multi-span simply supported; MSC, multi-span continuous; PSC, pre-stressed concrete; RC, reinforced concrete.

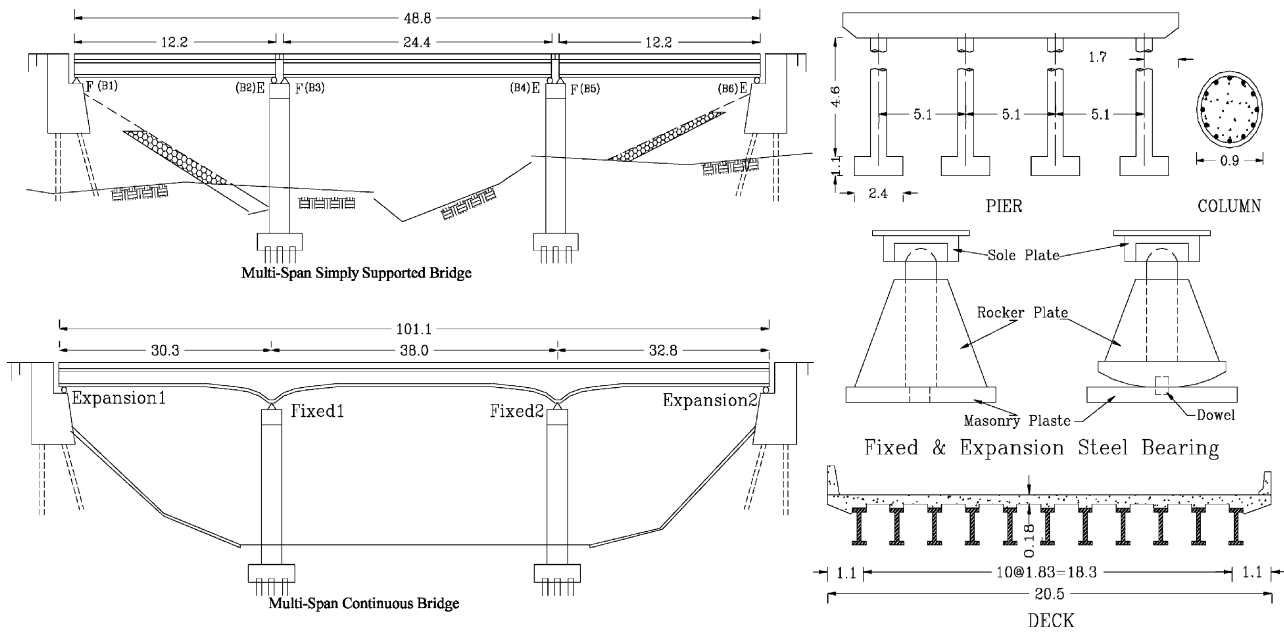


Fig. 1. Typical multi-span simply supported and multi-span continuous steel girder bridge in the Central and Southeastern United States.

ply supported spans supported on multi-column bents. There are four columns in a bent and 11 girders in a deck. The connection of the girder to the bent consists of elastomeric bearing pads with dowel bars projecting 9 in. into the cap and 6 in. up into holes cast in the bottom of the pre-cast girder ends as shown in Fig. 2. The general properties and dimensions of the concrete bridge are the same as those of the multi-span simply supported steel girder bridge given in the section above. However, the weight of the pre-stressed concrete girders is higher than that of the steel girders.

2.4. Multi-span continuous pre-stressed concrete girder bridge

The multi-span continuous pre-stressed concrete girder bridge (MSC-PSC) is similar to the MSSS-PSC, except that the superstructure is made continuous by either casting a parapet between the girders or making the deck continuous as seen in Fig. 2. This eliminates the intermediate expansion joints leaving gaps only at the abutments.

All the multi-span bridges have similar substructures consisting of multi-column bents. The columns for the bridges in this study are 914 mm (36 in) in diameter and have a 1% vertical reinforcing ratio with 10 mm (#3) or 12 mm (#4) circular ties spaced at 305 mm (12 in) vertically. The column vertical bars are spliced at the top of the footing with dowels projecting from the pile cap. The abutment is a stub abutment as designed in the AASHTO specifications with an expansion joint between the deck slab and abutment.

3. Analytical modeling of typical bridges

The four types of bridges discussed above consist of elements that may exhibit highly nonlinear behavior, such as the steel or elastomeric bearings, columns, abutments, and the impact between the decks. These nonlinearities are incorporated into two-dimensional nonlinear analytical models of the bridges. These models are developed using DRAIN-2DX [15].

The superstructure is modeled using linear beam-column elements, since the superstructure is expected to remain elastic under the seismic loads applied in the longitudinal direction. The stiffness assigned to the superstructure is that of the composite reinforced concrete deck and girder system. It should be noted that the stiffness of the superstructure does not have a significant effect on the seismic response of the bridge since the longitudinal response is typically governed by the bearings, columns, abutments, and foundation. Fig. 3 shows a schematic of the analytical model.

The columns are modeled using the DRAIN-2DX fiber element. Each fiber element has its own stress-strain relationship, and can be used to discretely model the cross-section of the column with its confined and unconfined concrete regions as well as the longitudinal steel reinforcement. A schematic of the fiber model is presented in Fig. 4 along with the moment curvature diagram for the columns. The yield curvature of this cross-section is 3.436×10^{-3} rad/m.

The steel fixed bearings, steel expansion bearings and concrete dowel bearings are modeled using truss and link elements, as shown in Figs. 5, 6 and 7,

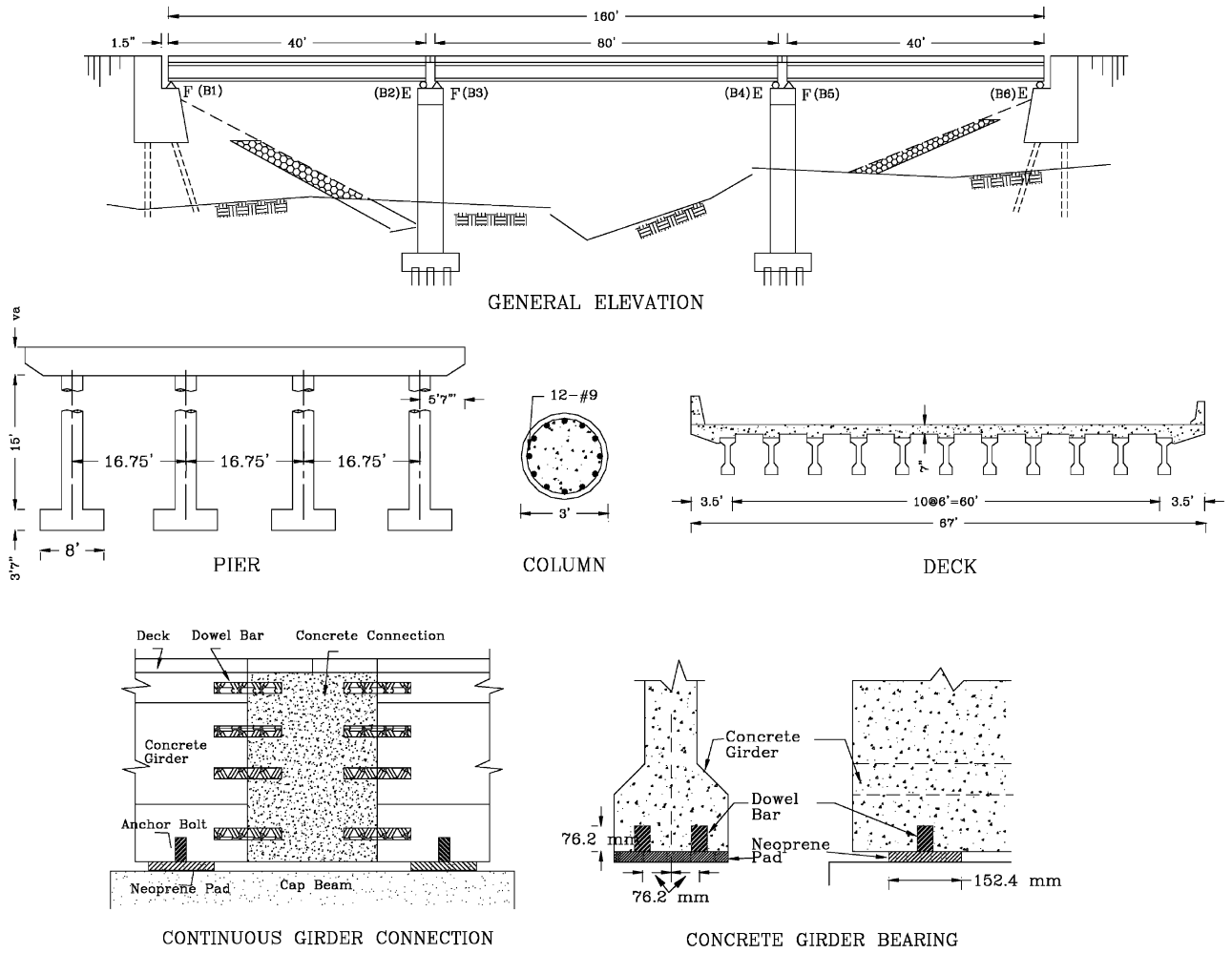


Fig. 2. Typical multi-span simply supported and multi-span continuous pre-stressed concrete girder bridge in the Central and Southeastern United States.

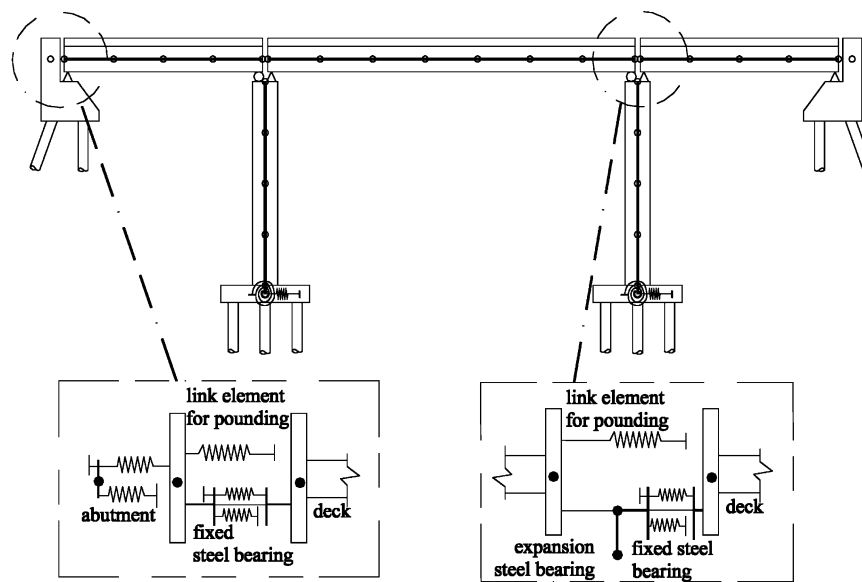


Fig. 3. Nonlinear analytical model of multi-span simply supported steel girder bridge including nonlinear elements used for the abutments, bearings, and columns.

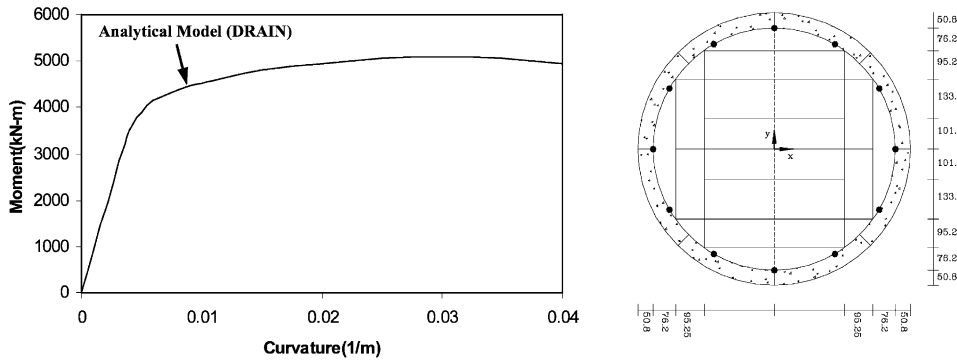


Fig. 4. Fiber model of reinforced concrete columns with moment-curvature of four columns in parallel.

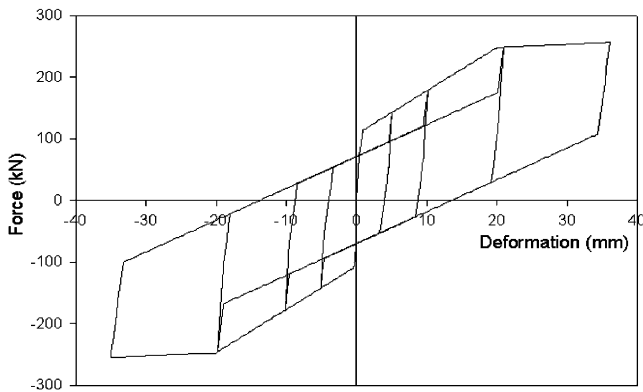


Fig. 5. Analytical model of fixed steel bearing.

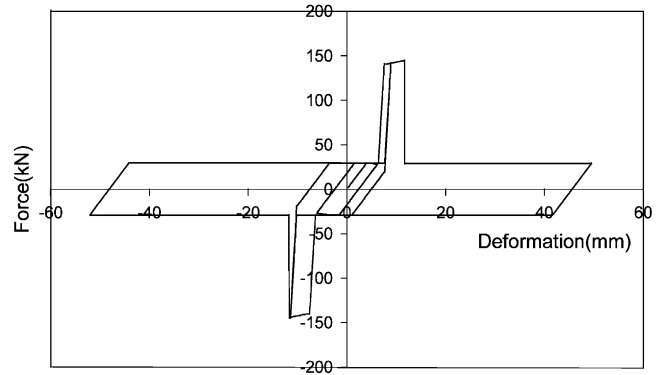


Fig. 7. Analytical model of bearing system for the pre-stressed concrete girders.

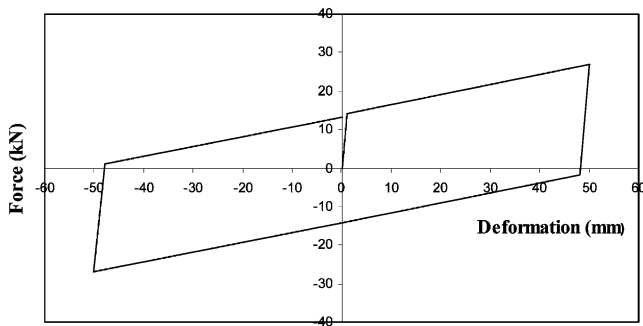


Fig. 6. Analytical model of expansion bearing.

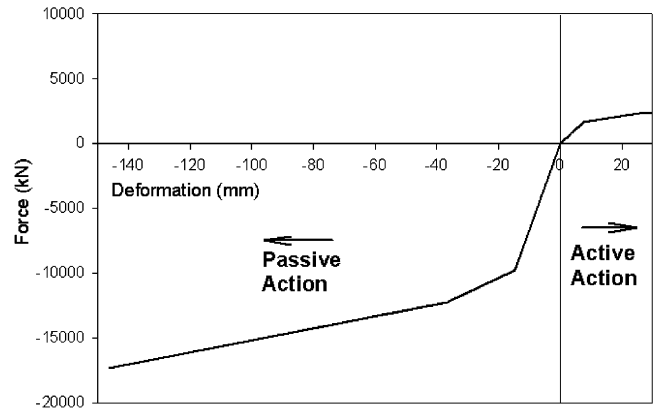


Fig. 8. Analytical model of abutment in passive and active action.

respectively. These models were developed based on previous tests of similar bearings [16].

The behavior of the abutment in both passive and active action as the bridge is loaded in the longitudinal direction is modeled by taking into account recommendations from Caltrans [17] as well as results of previous tests [18]. The analytical model for the abutments is shown in Fig. 8.

Pounding between deck slabs can affect the response of the bridge bearings significantly and therefore must be included as part of the bridge model. Pounding is modeled using a tri-linear compression only link

element with a gap to represent the expansion joint. The pounding model is given in Fig. 9 where $K_3 = 8.76 \times 10^3$ kN/mm, $K_2 = 1/2 K_3$, and $K_1 = 1/3 K_3$.

The pile foundations are modeled using a combination of linear translational and rotational springs. The horizontal and rotational stiffness of the foundations for the MSSS-SG, MSSS-PSC girder and MSC-PSC girder bridges is 547 kN/mm and 5.60×10^6 kN m/rad, respectively, whereas the stiffness for

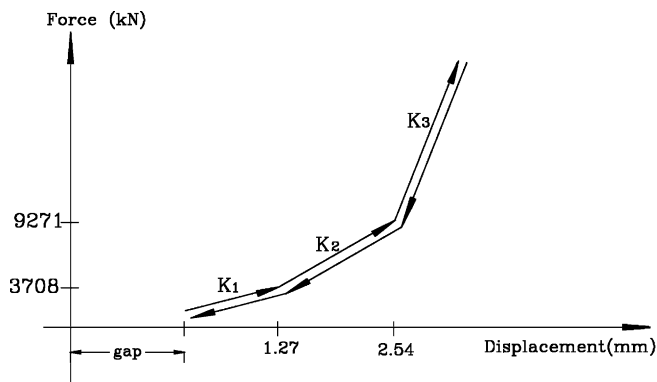


Fig. 9. Analytical model for pounding between decks.

the MSC-SG bridge foundation is 820 kN/mm and 1.04×10^7 kN m/rad, respectively.

4. Input ground motion simulation

Since few recorded strong ground motion records in the Southeastern and Central United States exist, a suite of synthetic ground motions developed by Hwang et al. [9] is used in this study. The suite consists of 100 ground motion records, distributed from weak to strong probabilistically and includes uncertainty in the soil and seismic characteristics. The peak ground acceleration of the ground motions ranges from 0.07 to 0.51 g. The range of moment magnitude is $M_w = 6.0$ – 8.0 , and the range of epicentral distance is 40–100 km. Fig. 10 shows the mean response spectra (MRS) and mean ± 1 standard deviation of the 100 ground motions and Fig. 11 shows the distribution of the ground motions at various peak ground acceleration levels.

The simulated ground motion records take into account the uncertainties in seismic source, path attenuation, and local soil conditions. Given a moment

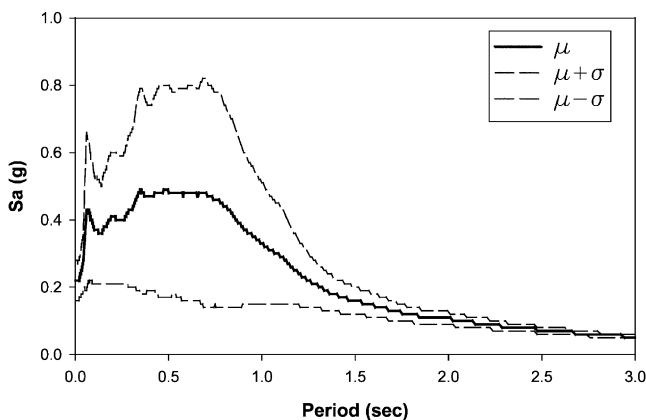


Fig. 10. Mean response spectrum and mean ± 1 standard deviation of the 100 ground motions.

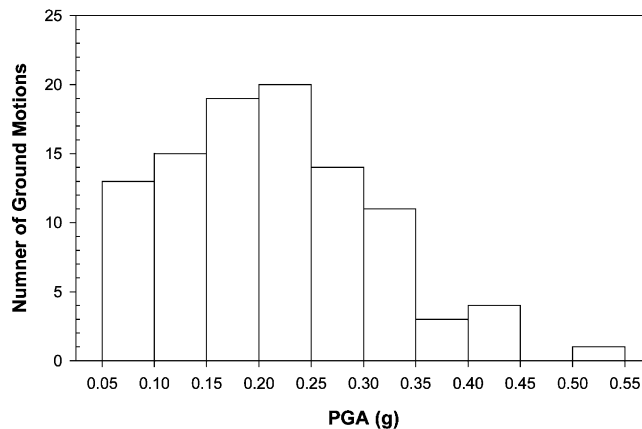


Fig. 11. Distribution of PGA of the 100 ground motions.

magnitude and epicentral distance, the uncertainties in the stress parameter, strong motion duration, cut-off frequency, and quality factor are also taken into account. The variability in the relative density of sand and the undrained shear strength of clay is considered in the site response analysis. The uncertainties in dynamic soil parameters, such as the shear modulus and damping ratio, are also included in the simulation.

5. Bridge model simulation

To represent the inherent variability in the material properties of steel and concrete, the uncertainties in the bridge strength and stiffness are included in the modeling of the four bridge types. The compressive strength of concrete and the yield strength of reinforcing steel are taken as random variables with a mean and standard deviation as recommended by Ellingwood and Hwang [19] and Mirza and MacGregor [20]. For each sample set, a cross-sectional analysis is performed to obtain the moment curvature relationship for the column sections to be used in the nonlinear analysis.

Previous studies have shown that the gap between the decks can have a significant effect on the response of the typical bridges [14]. Using the variation in temperature, and the coefficient of thermal expansion for steel and concrete, variabilities in gap size are obtained. The gap size is assumed to be normally distributed with a mean and standard deviation that is a function of the bridge type.

Using the Latin Hypercube sampling technique [21], a set of 10 nominally identical but statistically different bridges were developed for each bridge type. Each bridge sample is matched with a soil profile sample, and 10 earthquake samples, resulting in a total of 100 earthquake-site-bridge samples for each bridge type.

6. Characterization of damage

Most studies on fragility analysis of bridges use column ductility as the primary damage measure. Park and Ang [22] suggested a damage index based on energy dissipation, and Hwang et al. [11] used the capacity/demand ratio of the bridge columns to develop fragility curves. In this study, damage states are defined for column ductility demand, steel fixed and expansion bearing deformations, and elastomeric bearing deformations. The damage state definitions used are based on recommendations from previous studies and results from experimental tests and follow the qualitative descriptions of the damage states as provided by HAZUS which are shown in Table 2 [25]. However, engineering judgment should be used when determining the damage states, as these vary depending on the type, age, and condition of the bridge.

The quantified damage states for the columns are described by the column curvature ductility and are based on tests of nonseismically designed columns similar to those found in the bridges in this study [23]. The curvature ductility ranges from $\mu=1.0$ to $\mu=7.0$ for damage states ranging from slight damage to complete damage, as shown in Table 3. The lap-slices at the base of the columns are taken into account in the definition of the damage states.

The damage states for the fixed and expansion bearing are based on a series of experimental tests of bearings similar to those in this study [16,24]. For the fixed bearing, the damage states range from a deformation of 1.0 mm for slight damage to a deformation of 40.0 mm for complete damage, as shown in Table 3. At a deformation of $\delta=6.0$ mm, minor cracks occur in the concrete pedestal, which is defined as moderate damage. Strength degradation is observed at $\delta=20.0$ mm,

which is defined as extensive damage.

Expansion bearings are vulnerable to toppling if the longitudinal displacement of the bridge deck is too large. The problem of instability and unseating is a function of the size of the bearings and the width of the supports. In this study, the four damage states for the instability and unseating of expansion bearings are based on a judgment of the allowable displacement of the expansion bearings and the typical seat width. Based on typical bearings and supports, displacements of 50 and 100 mm are defined as slight and moderate damage, respectively. Extensive and complete damage are based on displacements of 150 and 255 mm, respectively. The damage states for the bearings in the pre-stressed concrete girder bridges are based on fracture of the bearing and the displacement necessary for unseating. The displacement at the complete damage state, $\delta=255$ mm, is based on the unseating of the PSC-girder (see Table 3).

7. Analytical fragility curves

The analytical fragility curves developed in this study are based on nonlinear response history analyses. First, a bridge is represented by an analytical model, which includes the inelastic behavior of the appropriate components (i.e. bearings and columns). Second, earthquake input motion for various characteristic magnitudes, epicentral distances, and local soil conditions is developed. Third, uncertainties in the modeling of seismic source, path attenuation, local soil conditions, and bridge components are quantified to establish a set of earthquake-bridge samples. Fourth, for each earthquake-bridge sample, a nonlinear response history analysis is performed. Using pre-determined damage indices, a damage state is assigned to each component of the bridge. Finally, using a probabilistic seismic demand model obtained by regression analysis on the simulated damage data, the individual fragility curves can be developed. Fig. 12 shows the results of the probabilistic seismic demand model for the components of the MSSS steel girder bridge having R^2 values in the range of 0.73–0.81.

A fragility curve describes the probability of reaching or exceeding a damage state as a function of a chosen ground motion intensity parameter (typically peak ground or spectral acceleration). In this study, five damage states are quantified in terms of the column curvature ductilities and the deformations of the fixed and expansion bearings. The probability that the demand on the structure exceeds the structural capacity can be computed as follows:

$$p_f = P \left[\frac{S_d}{S_c} \geq 1 \right] \quad (1)$$

Table 2
Description of bridge damage states (taken from HAZUS 97)

Damage states	Description
No damage (N)	No damage to a bridge
Slight/minor damage (S)	Minor cracking and spalling to the abutment, cracks in shear keys at abutments, minor spalling and cracks at hinges, minor spalling at the column (damage requires no more than cosmetic repair) or minor cracking to the deck
Moderate damage (M)	Any column experiencing moderate cracking and spalling (column structurally still sound), any connection having cracked shear keys or bent bolts, or moderate settlement of the approach
Extensive damage (E)	Any column degrading without collapse (column structurally unsafe), any connection losing some bearing support, or major settlement of the approach
Complete damage (C)	Any column collapsing and connection losing all bearing support, which may lead to imminent deck collapse

Table 3
Definition of damage states for bridge components

Damage state	Slight damage	Moderate damage	Extensive damage	Complete damage
Columns (μ)	$1.0 < \mu < 2.0$	$2.0 < \mu < 4.0$	$4.0 < \mu < 7.0$	$7.0 < \mu$
Steel bearings (δ , mm)	$1 < \delta < 6$	$6 < \delta < 20$	$20 < \delta < 40$	$40 < \delta$
Expansion bearings (δ , mm)	$\delta < 50$	$50 < \delta < 100$	$100 < \delta < 150$	$150 < \delta < 255$
Fixed dowels (δ , mm)	$8 < \delta < 100$	$100 < \delta < 150$	$150 < \delta < 255$	$255 < \delta$
Expansion dowels (δ , mm)	$\delta < 30$	$30 < \delta < 100$	$100 < \delta < 150$	$150 < \delta < 255$

where p_f is the probability of exceeding a specific damage state, S_d is the structural demand and S_c is the structural capacity.

If the structural capacity and seismic demand are described by a log-normal distribution, the probability of reaching or exceeding a specific damage state will be log-normally distributed, which can be obtained by a log-normal cumulative probability density function as follows:

$$P_f = \Phi \left[\frac{\ln(S_d/S_c)}{\sqrt{\beta_d^2 + \beta_c^2}} \right] \quad (2)$$

where β_c is the logarithmic standard deviation for the capacity, β_d is the logarithmic standard deviation for the demand, and $\Phi[\cdot]$ is the standard normal distribution function. The seismic demand is expressed as

$$\ln(S_d) = a \ln(x) + b \quad (3)$$

where a and b are unknown regression coefficients, and x is the ground motion intensity parameter (typically PGA or S_a). The composite logarithmic standard deviation $(\beta_d^2 + \beta_c^2)^{1/2}$, known as the dispersion, is taken

from values recommended in HAZUS 97 [25]. It should be noted that even though the probabilistic seismic demand model is performed for a peak ground acceleration range of 0.07–0.51 g, assuming a log-normal fit for the fragility curves allows extrapolation beyond this range within reason.

8. Component fragility curves

Fig. 13 shows the fragility curves for the various components of the multi-span simply supported steel girder bridge. Each of the components in the bridge (columns, fixed bearings and expansion bearings) has several subcomponents (columns 1 and 2, fixed bearings 1–3, etc.). To determine the fragility for each component, the most vulnerable subcomponent (i.e. largest fragility curve) is used. For example, for this bridge, column 1 controls for the columns, fixed bearing 1 for the fixed bearings and expansion bearing 1 for the expansion bearings. Similar fragilities were generated for the components of the MSC-PSC girder bridge, the MSC-SG bridge and the MSSS-PSC girder bridge.

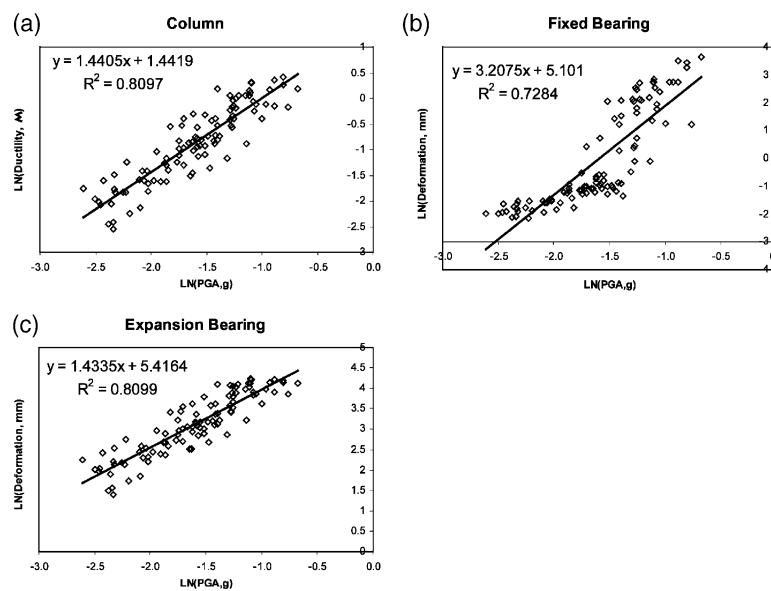


Fig. 12. Regression of the probabilistic seismic demand model of the MSSS-SG bridge for: (a) columns, (b) fixed steel bearings, (c) expansion steel bearings.

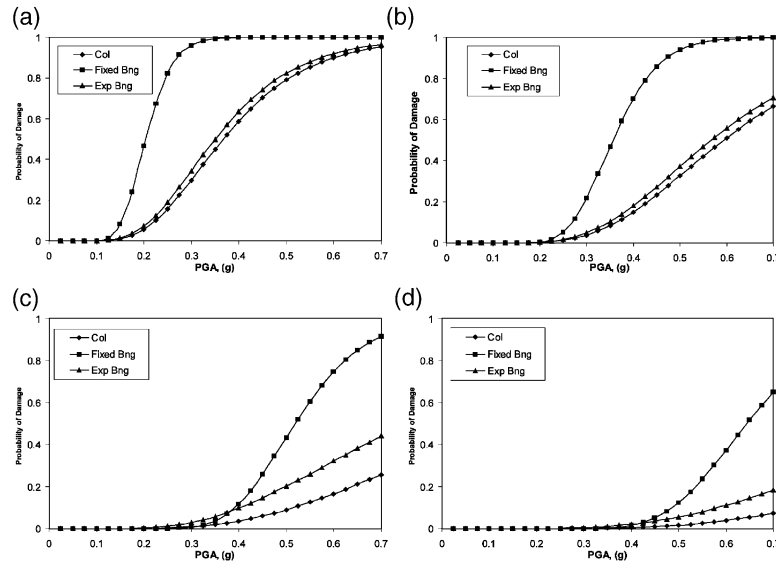


Fig. 13. Fragility curves for the various components of the MSSS-SG bridge for: (a) slight damage, (b) moderate damage, (c) extensive damage, and (d) complete damage.

It can be seen from Fig. 13 that the steel fixed bearing is the most fragile component in the multi-span simply supported steel girder bridge at all the damage states. This trend varies for different bridge types. For example, the columns for the multi-span continuous pre-stressed concrete girder bridge are the most fragile for the moderate, extensive and complete damage states. This indicates that it is important to include all major components when doing a fragility analysis of a bridge. If the assumption was made that the column damage states were representative of the damage states of the entire bridge, it is likely that this would result in an underestimation of the overall bridge system fragility.

9. Combining fragility curves

To enable comparison of various bridge types, it is essential that the overall bridge fragility be determined. This can be performed through a crude Monte-Carlo simulation but it is considerably more expensive computationally than the simulation performed in this study. An alternative would be to combine the component fragility curves to get the system (bridge) fragility curve. This, however, requires information about the stochastic dependence between the bridge components at various damage states.

Using first-order reliability theory, an upper and lower bound on the system fragility can be easily determined. The lower bound is the maximum component fragility while the upper bound is a combination of the component fragilities. These bounds are given in Eq. (4) where $P(F_i)$ is the probability of failure for each

component and $P(F_{\text{sys}})$ is the probability of failure for the entire system.

$$\max_{i=1}^m [P(F_i)] \leq P(F_{\text{sys}}) \leq 1 - \prod_{i=1}^m [1 - P(F_i)] \quad (4)$$

These first-order bounds are valid for a series type system which is where a failure of one of the components constitutes a failure of the system [26]. When a bridge is modeled in the longitudinal direction as in this study, it in fact behaves like a series system as seen in Fig. 3. The lower bound represents the probability of failure for a system whose components are all fully stochastically dependent and provides an un-conservative estimate for the fragilities of the subject bridges. The upper bound assumes that the components are all statistically independent and provides a conservative estimate on the overall bridge fragility. As the difference between the upper and lower bound decreases, the upper bound estimate of the system fragility becomes more appropriate.

The upper and lower bounds of the fragility curves for the MSSS steel girder bridge and the MSC steel girder bridge are shown in Figs. 14 and 15, respectively. The median peak ground acceleration values for all four bridge types are given in Table 4. The upper bound for the MSSS steel girder bridge has a median value of 0.19 g while the lower bound has a median of 0.20 g at the slight damage state. This same bridge type has upper and lower bounds of 0.47 and 0.52 g, respectively, for the extensive damage state which is the largest interval for the MSSS steel girder bridge at 0.05 g. The other three bridge types have fragility curves with bounds that are similar to those of the MSSS steel girder bridge for the slight damage state. The width of

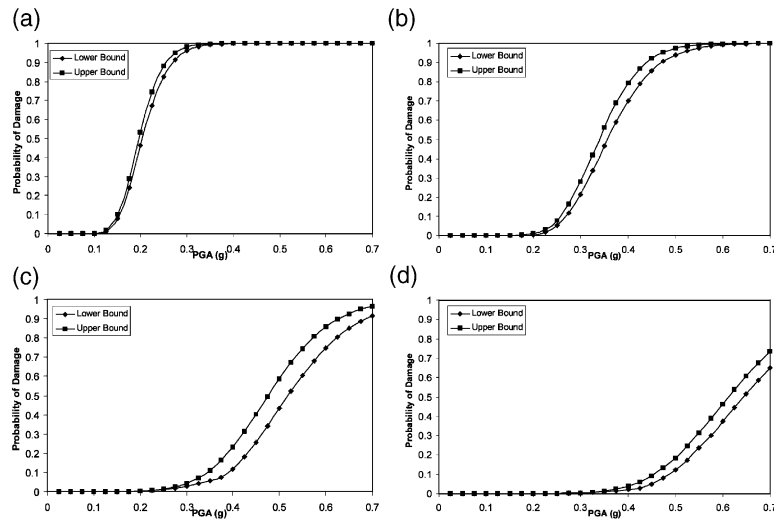


Fig. 14. First-order bounds for the MSSS-SG bridge for: (a) slight damage, (b) moderate damage, (c) extensive damage, and (d) complete damage.

the bounds increases as the damage state increases with the MSC concrete girder bridge showing the largest fragility curve bounds, as shown in Table 4. The bridge fragility curves that are used for further discussion in this paper are presented in Fig. 16 which are the first-order upper bounds of the individual bridge types.

The width of the bounds is governed by the relative fragility of each of the bridge components that are considered. If all the bridge components have similar fragilities, then the width of the first-order bounds is quite large, whereas if one component is considerably more fragile than the others, then the bounds are quite narrow. For instance, as in the case of the slight damage state for the MSSS-SG bridge, the fixed bearings are

considerably more fragile than any of the other components as seen in Fig. 13a and this results in the narrow bounds which are seen in Fig. 14a.

10. Results

Fig. 16 shows the upper bound approximation to the fragility curves for the four typical bridge types. This figure shows that the fragility curves for the various bridges have similar shapes, but with varying values for the different damage states. To allow comparisons of the vulnerability of the typical bridges, the median value of the probability of exceedance is determined for

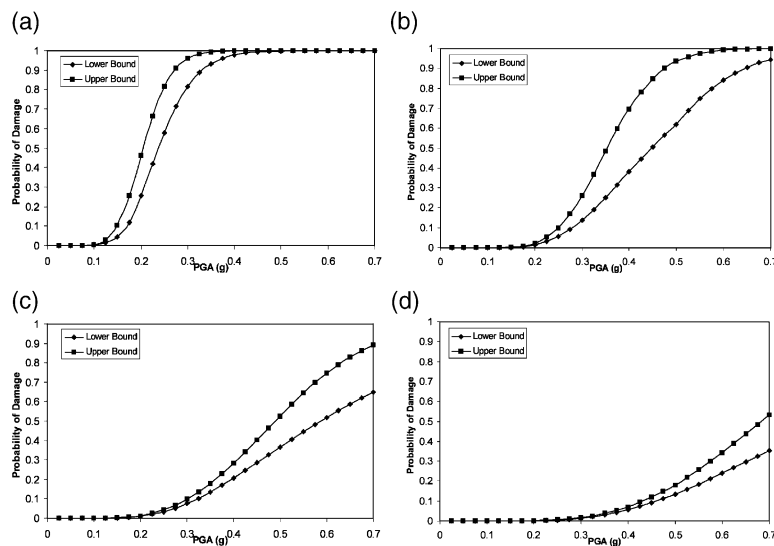


Fig. 15. First-order bounds for the MSC-SG bridge for: (a) slight damage, (b) moderate damage, (c) extensive damage, and (d) complete damage.

Table 4
Median values for upper and lower bounds of bridge fragility curves

Bridge type	Slight damage		Moderate damage		Extensive damage		Complete damage	
	Lower bound	Upper bound	Lower bound	Upper bound	Lower bound	Upper bound	Lower bound	Upper bound
MSSS steel	0.20	0.19	0.35	0.33	0.52	0.47	0.65	0.61
MSSS concrete	0.23	0.20	0.68	0.56	0.87	0.77	1.23	1.14
MSC steel	0.24	0.20	0.43	0.34	0.59	0.48	0.84	0.69
MSC concrete	0.25	0.24	1.57	1.31	2.61	2.01	4.54	3.47

each bridge and damage state. The median peak ground acceleration for each bridge at each damage state is given with its corresponding dispersion value in Table 5.

Fig. 17 shows a plot of the peak ground acceleration for the median values of probability of damage for the four damage states in this study. For the slight damage state, the median peak ground accelerations for the four bridge types range from 0.19 g for the MSSS steel girder bridge to 0.24 g for the MSC pre-stressed concrete girder bridge. For all four bridge types, the controlling component was the fixed bearings.

For the moderate damage state, the MSSS and MSC steel girder bridges have similar values of median peak ground acceleration of approximately 0.33 g. These bridge types are considerably more vulnerable than their pre-stressed concrete girder counterparts. The MSSS-PSC girder bridge has a median value of 0.56 g while the MSC-PSC girder bridge has a median peak ground acceleration of 1.31 g. For the MSSS-SG bridge, the fixed bearings are once again the most vulnerable components as shown in Fig. 13b. For the other three bridge types, the individual components

approximately contribute equally to the overall fragility of the bridges.

For the extensive damage state, the MSSS and MSC steel girder bridges are the most vulnerable with a median peak ground acceleration of approximately 0.47 and 0.48 g, respectively. These are followed by the MSSS and MSC pre-stressed concrete girder bridges which have median values that are approximately 0.77 and 2.01 g, respectively. For this damage state, the expansion bearings appear to control for the MSSS-PSC girder, MSC-PSC girder and MSC-SG bridges while the fixed bearing controls for the MSSS-SG bridge.

For the complete damage state, the median peak ground acceleration ranges from approximately 0.61 g for the MSSS steel girder bridge to 3.47 g for the MSC pre-stressed concrete girder bridge. The results of this analysis confirm previous results that have shown that the MSSS steel bridge is the most vulnerable of the typical bridge types [4]. It should be noted that the fragility curves were generated using synthetic ground motions that ranged from 0.07 to 0.51 g. While the log-normal assumption allows for extrapolation of the fragility curves beyond 0.51 g, it is understood that

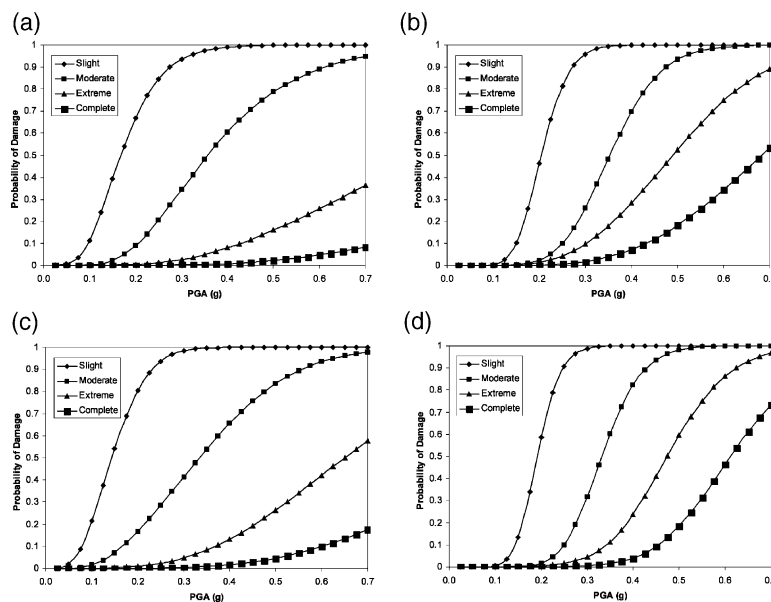


Fig. 16. Fragility curves for the typical bridges (a) MSC-PSC, (b) MSC-SG, (c) MSSS-PSC, (d) MSSS-SG.

Table 5
Fragility curve median values of typical bridges for peak ground acceleration

Bridge type	Slight damage		Moderate damage		Extensive damage		Complete damage	
	Median (g)	Displacement (b)	Median (g)	Displacement (b)	Median (g)	Displacement (b)	Median (g)	Displacement (b)
MSSS steel	0.20	0.19	0.33	0.21	0.47	0.23	0.61	0.25
MSSS concrete	0.20	0.31	0.56	0.35	0.77	0.42	1.14	0.44
MSC steel	0.20	0.21	0.34	0.25	0.48	0.34	0.69	0.38
MSC concrete	0.24	0.51	1.31	0.49	2.01	0.57	3.47	0.59

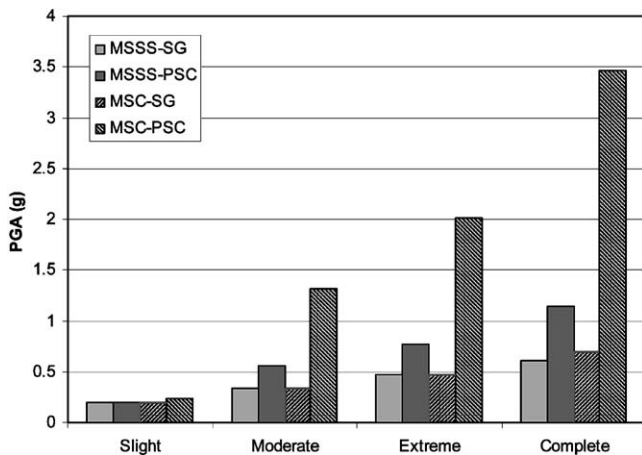


Fig. 17. Comparison of the median values of PGA for four typical bridge types found in mid-America.

accuracy at the large peak ground accelerations, such as those in the MSC-PSC girder bridge, is reduced. This, however, shows the general trend that the MSC-PSC girder bridge is the least vulnerable bridge type.

11. Conclusions

This study presents the development of fragility curves for bridges commonly found in the Central and Southeastern United States. The fragility curves that are presented are first-order approximations to the actual bridge fragility curves and were generated analytically by modeling the bridges in the longitudinal direction. These curves may be improved upon as more information is collected on the individual responses of the various bridge components in both the longitudinal and transverse directions. The components included in this study are the columns, fixed bearings and expansion bearings. Future studies should seek to include the abutments and the foundations.

These fragility curves can be used in determining the potential losses resulting from earthquakes and can be used to assign prioritization for retrofiting. The results show that the multi-span simply supported and the multi-span continuous steel girder bridges are the most vulnerable bridge types, based upon their median

values of peak ground acceleration for the various damage states. The median peak ground acceleration for complete damage for the MSSS-SG bridge and MSC-SG bridge is approximately 0.61 and 0.70 g, respectively. This is due to the steel fixed and rocker bearings typically used in these bridges, which have been shown to have poor seismic behavior.

The MSSS and MSC pre-stressed concrete girder bridges are less vulnerable compared with the MSSS and MSC steel girder bridges. The median peak ground acceleration for the complete damage state for the MSSS-PSC and MSC-PSC bridges is approximately 1.14 and 3.47 g, respectively. It is interesting to note that the continuity in the MSC-PSC girder bridge increases the seismic resistance on the bridge for the higher damage states compared with the MSSS-PSC girder bridge. This supports the common practice of making the pre-stressed concrete girders continuous in order to reduce the dead and live load moments and to reduce the maintenance required at the joints.

Acknowledgements

This study has been supported by the Earthquake Engineering Research Centers program of the National Science Foundation under Award Number EEC-9701785 (Mid-America Earthquake Center). The authors would like to thank Drs. Bruce Ellingwood, Howard Hwang and Y. K. Wen for their valuable comments throughout this project.

References

- [1] Chang KC. Seismic performance of highway bridges. *Earthquake Engineering and Engineering Seismology* 2000;2(1):55–77.
- [2] Japan Society of Civil Engineers. The 1999 Ji-Ji earthquake, Taiwan—investigation into the damage to civil engineering structures. Available from: <http://www.jsce.or.jp/e/index.html>.
- [3] Comartin C, Green M, Tubbesing S. The Hyogo-Ken Nanbu earthquake. Preliminary Reconnaissance Report, Earthquake Engineering Research Institute, Oakland (CA), February 1995.
- [4] Bruneau M, Wilson JC, Tremblay R. Performance of steel bridges during the 1995 Hyogo-Ken Nanbu (Kobe, Japan) earthquake. *Canadian Journal of Civil Engineering* 1996;23(3):678–713.

- [5] Moehle JP. Northridge earthquake of January 17, 1994: reconnaissance report, volume 1—highway bridges and traffic management. *Earthquake Spectra* 1994;11(3):287–372.
- [6] Buckle IG, editor. The Northridge California earthquake of January 17, 1994: performance of highway bridges. NCEER-94-0008, National Center for Earthquake Engineering Research, Buffalo (NY), March 24, 1994.
- [7] Basoz NI, Kiremidjian AS, King SA, Law KH. Statistical analysis of bridge damage data from the 1994 Northridge, CA earthquake. *Earthquake Spectra*, EERI 1999;15(1):25–53.
- [8] Shinozuka M, Feng MQ, Lee J, Naganuma T. Statistical analysis of fragility curves. *Journal of Engineering Mechanics*, ASCE 2000;126(12):1224–31.
- [9] Hwang H, Liu J, Chiu Y. Seismic fragility analysis of highway bridges. Center for Earthquake Research and Information, The University of Memphis, Memphis (TN), 38152.
- [10] Karim KR, Yamazaki F. Effect of earthquake ground motions on fragility curves of highway bridge piers based on numerical simulation. *Earthquake Engineering and Structural Dynamics* 2001;30:1839–56.
- [11] Hwang H, Jernigan JB, Lin Y. Evaluation of seismic damage to Memphis bridges and highway systems. *Journal of Bridge Engineering*, ASCE 2000;5(4):322–30.
- [12] Mander JB, Basoz N. Seismic fragility curve theory for highway bridges. Technical Council on Lifeline Earthquake Engineering Monograph, ASCE, New York (NY), vol. 16, 1999. p. 31–40.
- [13] Shinozuka M, Feng MQ, Kim H, Kim S. Nonlinear static procedure for fragility curve development. *Journal of Engineering Mechanics*, ASCE 2000;126(12):1287–95.
- [14] Choi E. Seismic analysis and retrofit of mid-America bridges. Ph.D. Thesis, Department of Civil and Environmental Engineering, Georgia Institute of Technology, Atlanta (GA), May 2002.
- [15] Prakash V, Powell GH, Campbell SD, Filippou FC. DRAIN-2DX user guide. Department of Civil Engineering, University of California, Berkeley, 1992.
- [16] Mander JB, Kim DK, Chen SS, Premus GJ. Response of steel bridge bearings to the reversed cyclic loading. Technical Report NCEER 96-0014, Buffalo (NY), 1996.
- [17] CALTRANS. Bridge design specifications manual. California Department of Transportation, 1990.
- [18] Maroney B, Kutter B, Romstad K, Cahi YH, Vanderbilt E. Interpretation of large scale bridge abutment test results. Proceedings of Third Annual Seismic Research Workshop, California Department of Transportation, June 27–29, 1994.
- [19] Ellingwood B, Hwang H. Probabilistic descriptions of resistance of safety-related structures in nuclear power plant. *Nuclear Engineering and Design* 1985;88:167–78.
- [20] Mizra S, MacGregor J. Variability of mechanical properties of reinforcing bars. *Journal of Structural Engineering*, ASCE 1979;105(5):921–37.
- [21] Ayyub BM, Lai K. Structural reliability assessment using latin hypercube sampling. Proceeding of ICOSSAR '89, the Fifth International Conference on Structural Safety and Reliability, San Francisco (CA), USA, 1989.
- [22] Park YJ, Ang AH-S. Mechanistic seismic damage model for reinforced concrete. *Journal of Structural Engineering*, ASCE 1985;111(4):722–39.
- [23] Dutta A. On energy based seismic analysis and design of highway bridges. Ph.D. Dissertation, Department of Civil, Structural and Environmental Engineering, State University of New York, Buffalo (NY), 1999.
- [24] Randall MJ, Saiidi MS, Maragakis EM, Isakovic T. Restraint design procedures for multi-span simply supported bridges. Technical Report MCEER-99-0011, 1999.
- [25] HAZUS. Earthquake loss estimation methodology. Technical Manual, National Institute of Building for the Federal Emergency Management Agency, Washington (DC), 1997.
- [26] Melchers RE. *Structural Reliability, Analysis and Prediction*, 2nd ed. John Wiley & Sons; 1999.